

Heat Source effects of flow past a parabolic accelerated isothermal vertical plate in the presence of Hall Current, Chemical reaction, Rotation and Radiation



D.Lakshmikaanth^{1,2} A.Selvaraj^{1,*} A.Neel Armstrong³

¹Department of Mathematics, Vels Institute of Science, Technology and Advanced Studies, Chennai-600117, India

*E-mail:aselvaraj_ind@yahoo.co.in

²College of Fish Nutrition & Food Technology, TNJFU, Chennai-600051, India

³Department of Mathematics, St. Eugene university, Lusaka, Zambia

Abstract: This is a study of Hall current, Heat Source with Radiation & Chemical reaction effects on First-order viscous fluid flow which is an incompressible fluid and we focus on heat and mass transfer past an accelerated isothermal vertical plate with Rotation. We employ Inverse Laplace Transform Technique to solve the ascendant mathematical equations. The numerical values are given after our study of the accelerated flow with respect to certain parameters like Thermal Grashof number, Prandtl number, Schmidt number, and Mass Grashof number. Based on the study we have deduced that, Velocity increases when Heat Source, Hall Current and Grashof Values rises, Velocity reduces when Radiation rises. Also, Temperature falls when radiation rises and temperature rises when Heat Source rises. Concentration reduces when chemical reaction increased.

Key words: Hall Current, Radiation, Rotation, Heat source, Chemical reaction.

1. Introduction

Movement of fluid subject to some unbalance forces plays an important role in the study of heat and Mass transfer in fluid dynamics. As this is needed to understand working of a wide range of systems like biological systems, home appliances, industrial operations, food preparation etc., this kind of study is an imperative one. [1] Is one such study which found out that velocity of the fluid decreases when increasing the Schmidt number and chemical reaction parameter? [2] Is another study which concludes that the velocity of fluid rises as 'time' and the velocity falls as the Prandtl number increases? [3] Is a study which found out that the velocity rises as Thermal Grashof, Chemical Reaction, time, and Mass Grashof values are increased? In addition, it also claims that as Pr and Sc increase as velocity reduces. [4] Found out that the axial velocity hiked as value of hall parameter, Mass and thermal Grashof number [5] concludes that the velocity rises as Grashof numbers are increased. Similar findings in literature show that as the rotational limit is lowered, speed increases. [6] Deduced the result that Concentration profile decreases with increasing Schmidt number. [7] is an analysis deducing how the parameters of the thermal Grashof values, Mass Grashof values, time and variable thermal conductivity cause rise in velocity while parameters like Prandtl, Schmidt, Radiation, chemical reaction and magnetic field

*Corresponding author: A.Selvaraj

cause velocity to decrease. [8] Gives a graphical estimation of temperature, float speed, and mindfulness. It is an interesting study which observes an executed attractive region's tendency edge increases as the speed decreases. [9] Theorizes that velocity rises as Gr and Gc rise. Also, as the Prandtl number rises, the temperature drops, and as the Schmidt number rises, the mass concentration rises. [10] Depicts the impacts of the non-uniform heat parameter on dynamic speed. The numerical technique on several parameters of heat radiation was obtained by [11]. [12] Is regarding The Hall current effect on unsteady hydro magnetic flow. [17] Observed that destructive reaction has a fall in velocity and concentration while the generative reaction has an increase. Inspired by the above we are pursuing the study of heat source effects where we observe fluid flow past a parabolic, accelerated, isothermal and vertical plate with respect to Hall current, chemical reaction, Rotation and radiation.

2. Numerical Formulation

Here, we assume viscous, incompressible fluid that conducts current flowing past an infinite plate that is located in the plane $z = 0$. The y-axis is normal to other axes, while x-axis is measured in the object's drift order. This plate is parabolic accelerated along the x-axis with a velocity of $q = t^2$. The plate in this instance is not electrically conductive. In the flow field, the pressure is uniform as well. The continuity equation if (u^*, v^*, w^*) denotes the elements of 'F' velocity vector. $w^* = 0$ is satisfied when $F = 0$ results in $w^* = 0$ everywhere in the flow. Here, just z and t determine the flow volumes, The following equations regulate the unsteady flow under these presumptions.

$$\frac{\partial u^*}{\partial t^*} - 2\Omega v^* = \rho \frac{\partial^2 u^*}{\partial z^{*2}} + g\beta(T^* - T_\infty^*) + g\beta(C^* - C_\infty^*) - \frac{\sigma B_0^2 \mu^2 (u^* + m_1 v^*)}{\rho(1+m_1^2)} \quad (1)$$

$$\frac{\partial v^*}{\partial t^*} + 2\Omega u^* = \rho \frac{\partial^2 v^*}{\partial z^{*2}} + \frac{\sigma B_0^2 \mu^2 (m_1 u^* - v^*)}{\rho(1+m_1^2)} \quad (2)$$

$$\frac{\partial \theta^*}{\partial t^*} = \frac{1}{P_r} \frac{\partial^2 \theta^*}{\partial z^{*2}} - R\theta^* + Q\theta^* \quad (3)$$

$$\frac{\partial C^*}{\partial t^*} = \frac{1}{S_c} \frac{\partial^2 C^*}{\partial z^{*2}} - kC^* \quad (4)$$

The boundary conditions are

$$u^* = 0, v^* = 0, T^* = T_\infty^*, C^* = C_\infty^* \text{ at } t_\infty^* \leq 0 \forall z_\infty^*$$

$$u^* = t^{*2}, T^* = T_\infty^*, C^* = C_\infty^* \text{ at } t^* > 0 \text{ for } z^* = 0(5)$$

$$u^* \rightarrow 0, T^* \rightarrow T_\infty^*, C^* \rightarrow C_\infty^* \text{ at } z_\infty^* \rightarrow \infty$$

The consequent dimensionless aggregate is

$$U = \frac{u^*}{(Vu_0)^{\frac{1}{3}}}, V = \frac{v^*}{(Vu_0)^{\frac{1}{3}}}, t = t^* \left(\frac{(u_0^2)}{v} \right)^{\frac{1}{3}}, Z = z^* \left(\frac{(u_0^2)}{v^2} \right)^{\frac{1}{3}}$$

$$\theta = \frac{T^* - T_\infty^*}{T_w^* - T_\infty^*}, G_r = \frac{g\beta(T_w^* - T_\infty^*)}{u_0}, C = \frac{C^* - C_\infty^*}{C_w^* - C_\infty^*}, G_c = \frac{g\beta(C^* - C_\infty^*)}{C_w^* - C_\infty^*} \quad (6)$$

$$Pr = \frac{\mu C_p}{k}, K = K_1 \left(\frac{v}{u_0^2} \right)^{\frac{1}{3}}, Sc = \frac{v}{D}, M^2 = \frac{\sigma B_0^2}{\rho} \left(\frac{v}{u_0^2} \right)^{\frac{1}{3}}$$

On suggesting non dimensional parameters, Pr, Sc, Gc, Gr ratios areas presented in equation. It is important to determine the values of thermal layer transfer and proportionate heat transfer when measuring velocity since Pr is the ratio between momentum and thermal diffusivity. The heat transfer known as the Grashof number calculates the buoyancy to viscosity ratio. Since the buoyant force, as opposed to the viscous force, is mostly responsible for the convection, it is appropriate to measure the fluid to demonstrate this.

To examine the diffusion coefficient, use Schmidt as the ratio between mass diffusivity and momentum. Ist order chemical reaction on flow past a parabolic with rotation is shown using coupled partial differential equations. Complex velocity $q = u + iv$ was used to solve eq. (1) and (2), which were then combined into one equation.

$$\frac{\partial q}{\partial t} = G_r \theta + G_c C + \frac{\partial^2 q}{\partial z^2} - mq \quad \text{where } m = \frac{M^2}{(1+hi)} - 2\Omega i \quad (7)$$

$$\frac{\partial \theta}{\partial t} = \frac{1}{Pr} \frac{\partial^2 \theta}{\partial z^2} - R\theta + Q\theta \quad (8)$$

$$\frac{\partial C}{\partial t} = \frac{1}{Sc} \frac{\partial^2 C}{\partial z^2} - kC \quad (9)$$

With conditions,

$$q = 0, \theta = 0, C = 0 \text{ for all } z, t \leq 0$$

$$q = t^2, \theta = 1, C = 1 \text{ for all } z, t = 0 \quad (10)$$

$$q \rightarrow 0, \theta \rightarrow 0, C \rightarrow 0 \text{ as } z \rightarrow \infty.$$

3.Elucidation of the Problem

Applying Inverse Laplace Technique to Solve eqn (7) to (9) using eqn (10)

$$\begin{aligned}
 q(z) = & \left\{ \begin{aligned} & \left[\frac{\eta^2 t}{m} + t^2 \right] \frac{1}{2} \left[\begin{aligned} & e^{-2\eta\sqrt{t}\sqrt{m}} \operatorname{erfc}(\eta - \sqrt{mt}) \\ & + e^{2\eta\sqrt{t}\sqrt{m}} \operatorname{erfc}(\eta + \sqrt{mt}) \end{aligned} \right] \\ & + \left[\frac{1}{4m} - t \right] \frac{2\eta\sqrt{t}}{2\sqrt{m}} \left[\begin{aligned} & e^{-2\eta\sqrt{t}\sqrt{m}} \operatorname{erfc}(\eta - \sqrt{mt}) \\ & - e^{2\eta\sqrt{t}\sqrt{m}} \operatorname{erfc}(\eta + \sqrt{mt}) \end{aligned} \right] \\ & - \frac{2}{m} \sqrt{\frac{t}{\pi}} e^{\left(\frac{-z^2}{4t} - mt\right)} \end{aligned} \right\} \\
 & - \frac{G_r}{a(1 - Pr)} \left\{ \begin{aligned} & \frac{e^{at}}{2} \left[\begin{aligned} & e^{-2\eta\sqrt{t}\sqrt{a+m}} \operatorname{erfc}(\eta - \sqrt{(a+m)t}) \\ & + e^{2\eta\sqrt{t}\sqrt{a+m}} \operatorname{erfc}(\eta + \sqrt{(a+m)t}) \end{aligned} \right] \\ & - \frac{1}{2} \left[\begin{aligned} & e^{-2\eta\sqrt{t}\sqrt{m}} \operatorname{erfc}(\eta - \sqrt{mt}) \\ & + e^{2\eta\sqrt{t}\sqrt{m}} \operatorname{erfc}(\eta + \sqrt{mt}) \end{aligned} \right] \end{aligned} \right\} \\
 & - \frac{G_s}{b(1 - Sc)} \left\{ \begin{aligned} & \frac{e^{at}}{2} \left[\begin{aligned} & e^{-2\eta\sqrt{t}\sqrt{b+m}} \operatorname{erfc}(\eta - \sqrt{(b+m)t}) \\ & + e^{2\eta\sqrt{t}\sqrt{b+m}} \operatorname{erfc}(\eta + \sqrt{(b+m)t}) \end{aligned} \right] \\ & - \frac{1}{2} \left[\begin{aligned} & e^{-2\eta\sqrt{t}\sqrt{m}} \operatorname{erfc}(\eta - \sqrt{mt}) \\ & + e^{2\eta\sqrt{t}\sqrt{m}} \operatorname{erfc}(\eta + \sqrt{mt}) \end{aligned} \right] \end{aligned} \right\} \\
 & + \frac{G_r}{a(1 - Pr)} \left\{ \begin{aligned} & \frac{e^{at}}{2} \left[\begin{aligned} & e^{-2\eta\sqrt{t}\sqrt{Pr(a+R-Q)}} \operatorname{erfc}(\eta\sqrt{Pr} - \sqrt{(a+R-Q)t}) \\ & + e^{2\eta\sqrt{t}\sqrt{Pr(a+R-Q)}} \operatorname{erfc}(\eta\sqrt{Pr} + \sqrt{(a+R-Q)t}) \end{aligned} \right] \\ & - \frac{1}{2} \left[\begin{aligned} & e^{-2\eta\sqrt{t}\sqrt{Pr(R-Q)}} \operatorname{erfc}(\eta\sqrt{Pr} - \sqrt{(R-Q)t}) \\ & + e^{2\eta\sqrt{t}\sqrt{Pr(R-Q)}} \operatorname{erfc}(\eta\sqrt{Pr} + \sqrt{(R-Q)t}) \end{aligned} \right] \end{aligned} \right\} \\
 & + \frac{G_c}{b(1 - Sc)} \left\{ \begin{aligned} & \frac{e^{bt}}{2} \left[\begin{aligned} & e^{-2\eta\sqrt{t}\sqrt{Sc(b+k)}} \operatorname{erfc}(\eta\sqrt{Sc} - \sqrt{(b+k)t}) \\ & + e^{2\eta\sqrt{t}\sqrt{Sc(b+k)}} \operatorname{erfc}(\eta\sqrt{Sc} + \sqrt{(b+k)t}) \end{aligned} \right] \\ & - \frac{1}{2} \left[\begin{aligned} & e^{-2\eta\sqrt{t}\sqrt{Sc k}} \operatorname{erfc}(\eta\sqrt{Sc} - \sqrt{kt}) \\ & + e^{2\eta\sqrt{t}\sqrt{Sc k}} \operatorname{erfc}(\eta\sqrt{Sc} + \sqrt{kt}) \end{aligned} \right] \end{aligned} \right\} \tag{11}
 \end{aligned}$$

$$\text{where } \eta = \frac{z}{2\sqrt{t}}, a = \frac{Pr(R-Q) - m}{1 - Pr} \quad \text{and} \quad b = \frac{kSc - m}{1 - Sc}$$

$$\theta = \frac{1}{2} \left[\begin{aligned} & e^{-2\eta\sqrt{Pr}\sqrt{(R-Q)t}} \operatorname{erfc}(\eta\sqrt{Pr} - \sqrt{(R-Q)t}) \\ & + e^{2\eta\sqrt{Pr}\sqrt{(R-Q)t}} \operatorname{erfc}(\eta\sqrt{Pr} + \sqrt{(R-Q)t}) \end{aligned} \right] \tag{12}$$

$$C = \frac{1}{2} \left[e^{-2\eta\sqrt{t}\sqrt{Sc}k} \operatorname{erfc}(\eta\sqrt{Sc} - \sqrt{kt}) + e^{2\eta\sqrt{t}\sqrt{Sc}k} \operatorname{erfc}(\eta\sqrt{Sc} + \sqrt{kt}) \right] \quad (13)$$

4. Results and Discussion

The outcome for varying values of Chemical Reaction k , Schmidt Number Sc , Prandtl Number Pr , Thermal Grashof Gr , Mass Grashof Gc , Hall current h , radiation R , Heat Source Q , Rotation w . The values are fixed and generated where ever necessary $k=1.0$, $Pr=7.0$, $Sc=2.01$, $Gr=7.0$, $Gc=7.0$, $h=2$, $R=5$ and $Q=1$.

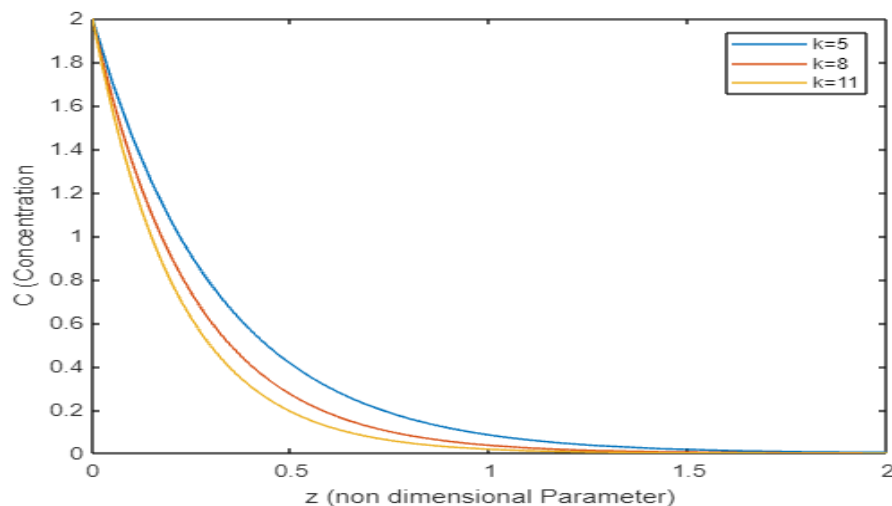


Fig 1: Concentration Profile for various values of Chemical Reaction k

It is clearly observable from the diagram that increase in the value k of the chemical reaction induces a decline in the concentration C and the same is true for all the three values experimented with $k = 5.0, 8.0, 11.0$

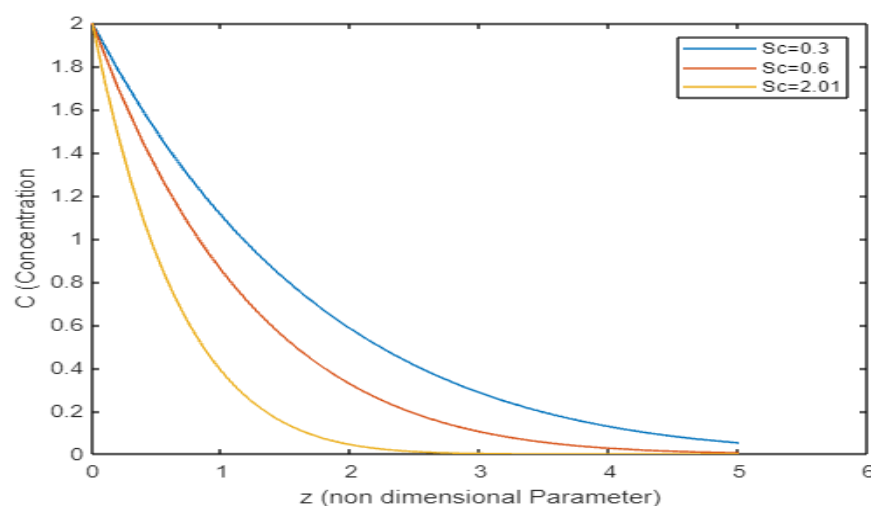


Fig 2: Concentration Profile for various values of Schmidt Number Sc .

It is clearly observable from the diagram that increase in the value of the Schmidt number induces a decline in the concentration C and the same is true for all the three values

experimented with, 0.3, 0.6 as well as 2.01.

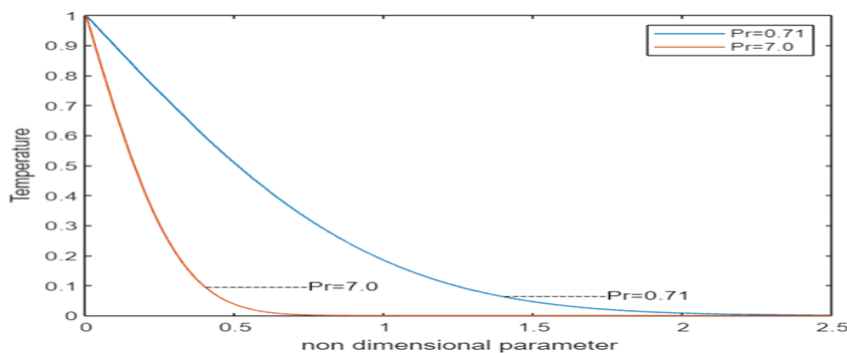


Fig 3 :Temperature Profile for various values of Prandtl Number Pr.

It is clearly observable from the diagram that the temperature for the liquid with the prandtl number 0.71 is more than that for the gas, Prandtl number 7 though they both are equal to start with in the initial value.

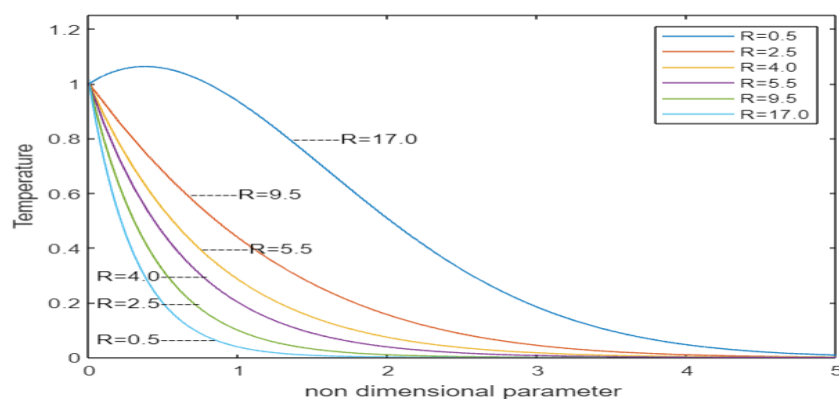


Fig 4 :Temperature Profile for various values of Radiation R.

It is clearly observable from the diagram that increase in the value of the Radiation induces increase in the Temperature T and the same is true for all the six values experimented with R= 0.5,2.5,4.0,5.5,9.5 and 17.0.

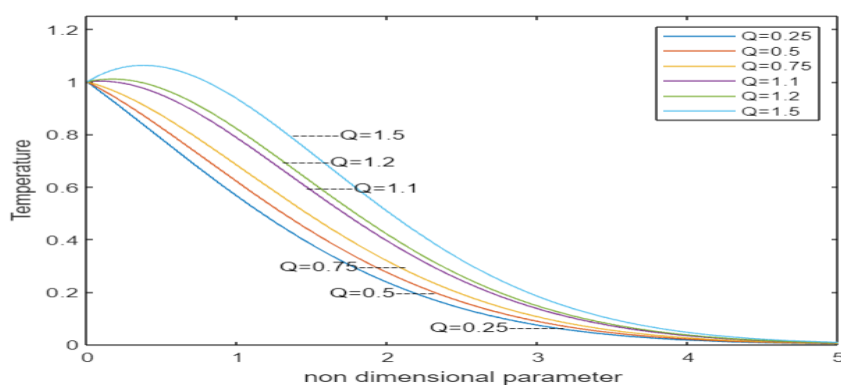


Fig 5 :Temperature Profile for distinct values of Heat Source Q

It is clearly observable from the diagram that increase in the value of the Heat Sources induces increase in the Temperature T and the same is true for all the six values experimented

with $Q = 0.25, 0.5, 0.75, 1.1, 1.2$ as well as 1.5.

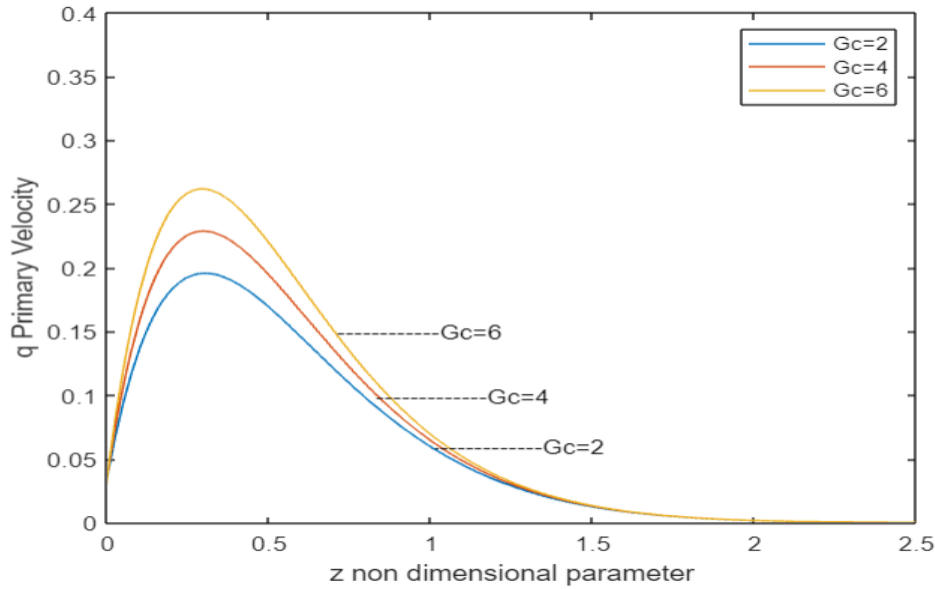


Fig 6 :Primary Velocity Profile for distinct values of Mass Grashof Number G_c

It is clearly observable from the diagram that increase in the value of Mass Grashof values induces increase in the Primary Velocity and the same is true for all the three values experimented With $G_c = 2, 4, 6$.

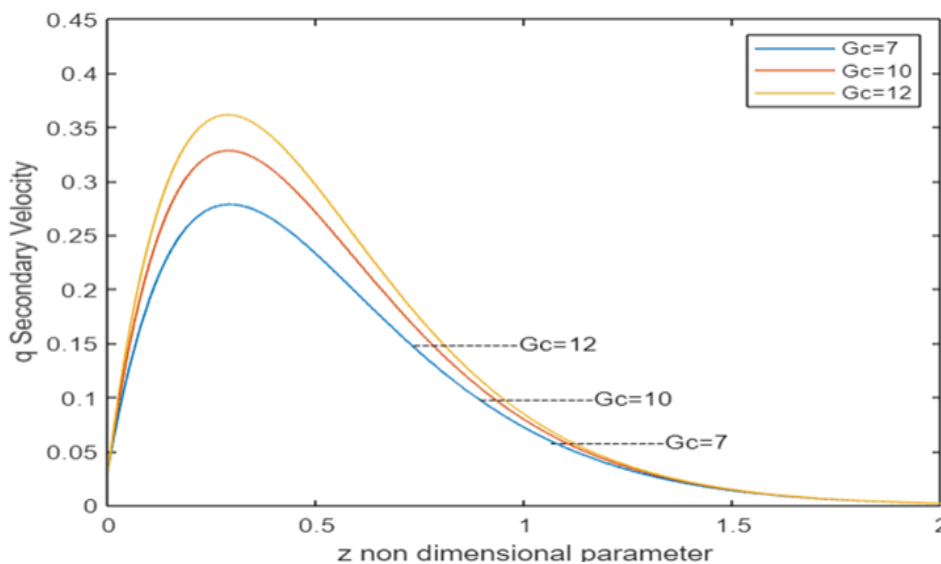


Fig 7 :Secondary Velocity Profile for distinct values of Mass Grashof Number G_c

It is clearly observable from the diagram that increase in the value of Mass Grashof values induces increase in the Secondary velocity and the same is true for all the three values experimented with $G_c = 7, 10, 12$.

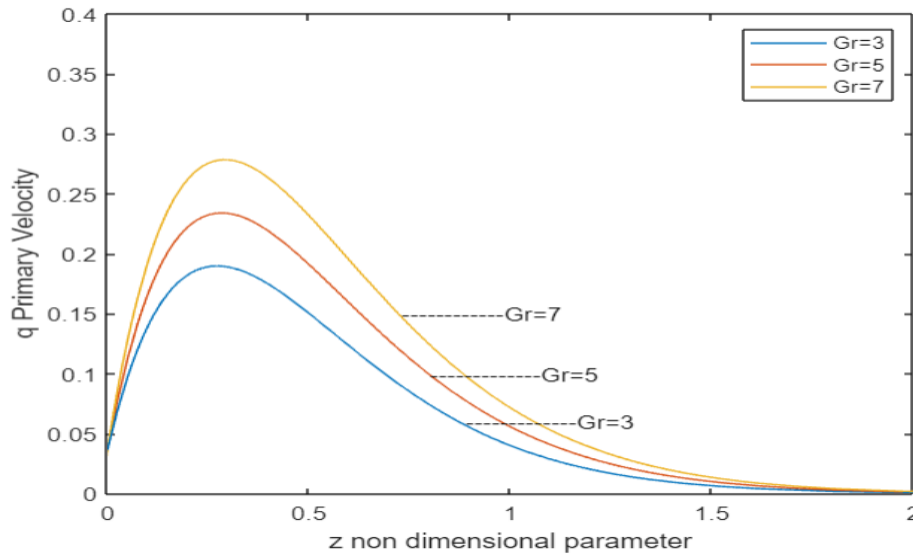


Fig 8 :Primary Velocity Profiles for the distinctive values of Grashof Thermal Gr

It is clearly observable from the diagram that increase in the value of Thermal Grashof values induces increase in the Primary Velocity and the same is true for all the six values experimented with $Gr = 3, 5, 7$.

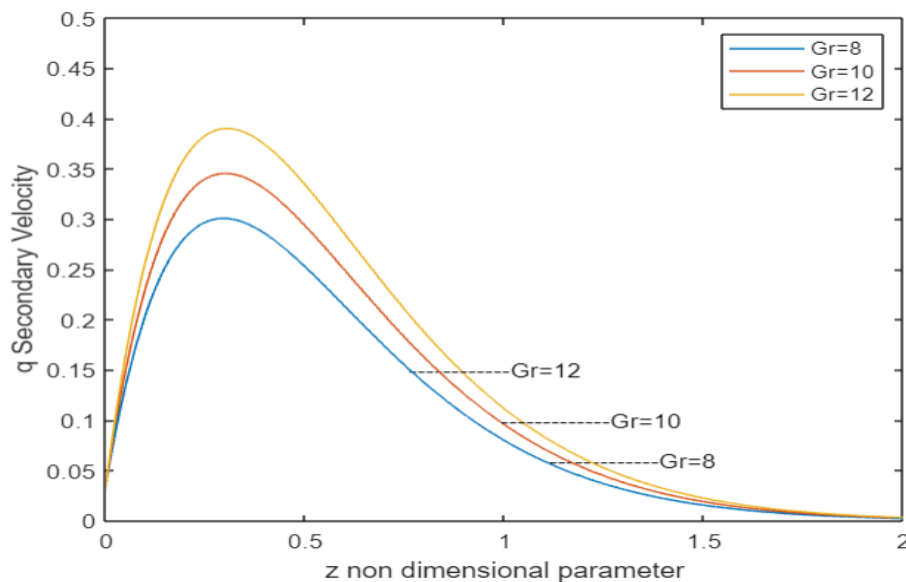


Fig 9 : Secondary Velocity Profiles for the distinctive values of Grashof Thermal Gr

It is clearly observable from the diagram that increase in the value of Thermal Grashof values induces increase in the Secondary velocity and the same is true for all the six values experimented with $Gr = 8, 10, 12$.

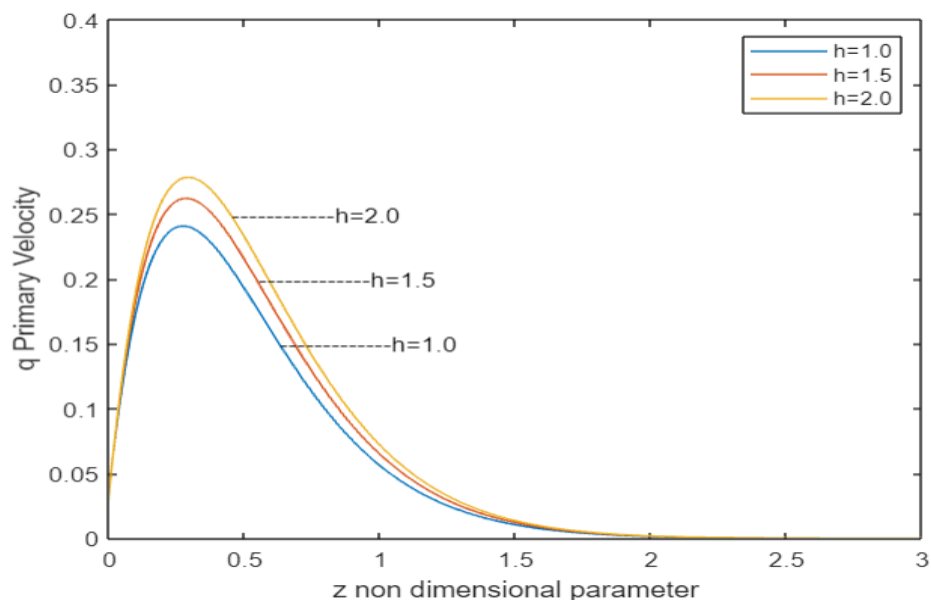


Fig 10 :Primary Velocity Profiles for the distinctive values of Hall Current h

It is clearly observable from the diagram that increase in the value of Hall current induces decline in the Primary Velocity as well as Secondary velocity and the same is true for all the six values experimented with, 1.0, 1.5, 2.0.

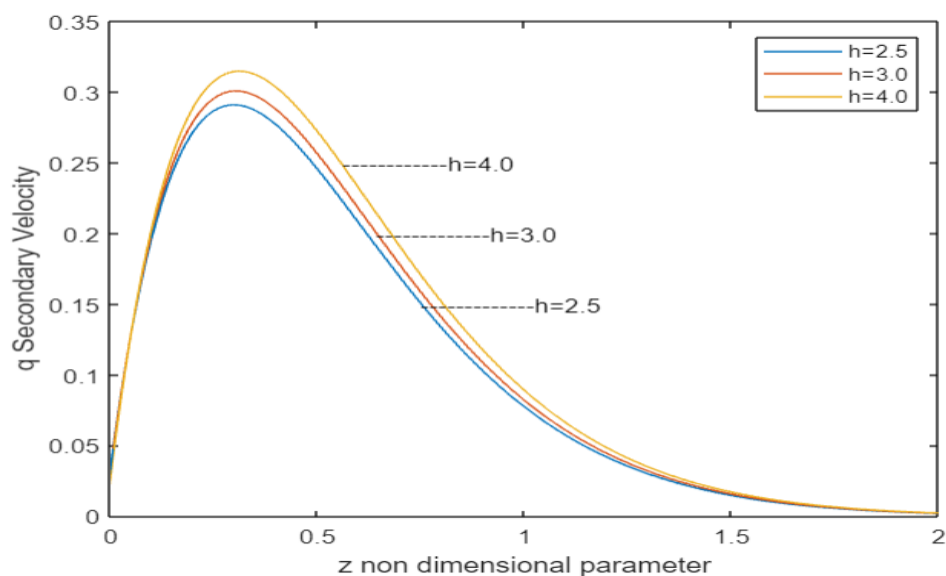


Fig 11 :Secondary Velocity Profiles for the distinctive values of Hall Current h

It is clearly observable from the diagram that increase in the value of Hall current induces decline in the Secondary velocity and the same is true for all the six values experimented with $h = 7.0, 10.0, 13.0$.

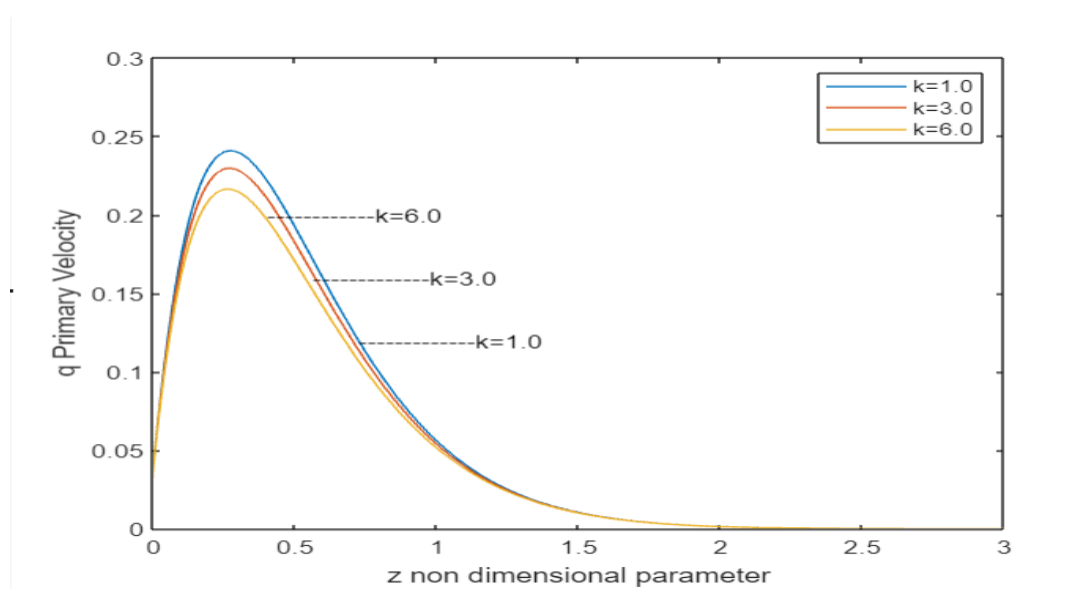


Fig 12 :Primary Velocity Profiles for the distinctive values of Chemical Reaction k .

It is clearly observable from the diagram that increase in the value of Chemical reaction k values induces declines in the Primary Velocity and the same is true for all the six values experimented with $k = 1.0, 3.0, 5.0$.

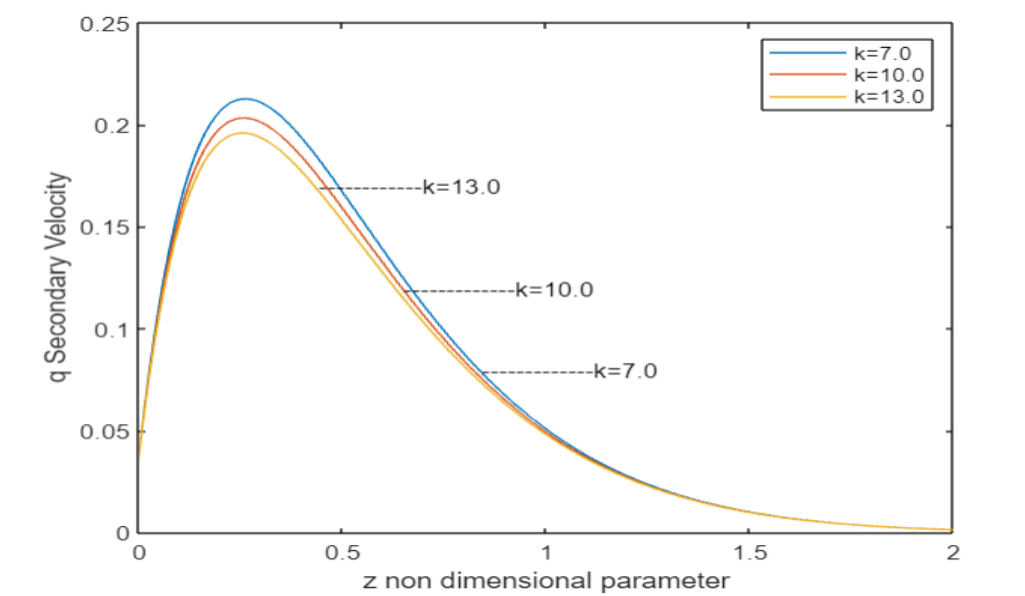


Fig 13 :Secondary Velocity Profiles for the distinctive values of Chemical reaction k

It is clearly observable from the diagram that increase in the value of Chemical reaction k values induces declines in the Secondary Velocity and the same is true for all the six values experimented with $k = 7.0, 10.0, 13.0$.

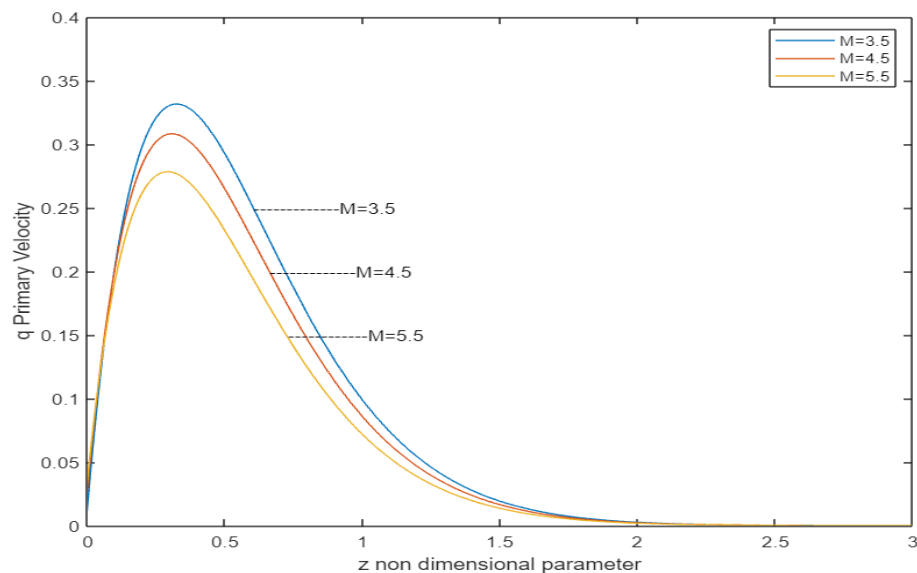


Fig 14: Primary Velocity Profiles for the distinctive values of Hartmann number M

It is clearly observable from the diagram that increase in the value of Hartmann number values induces increase in the Primary Velocity and the same is true for all the six values experimented with $M = 3.5, 4.5, 5.5$.

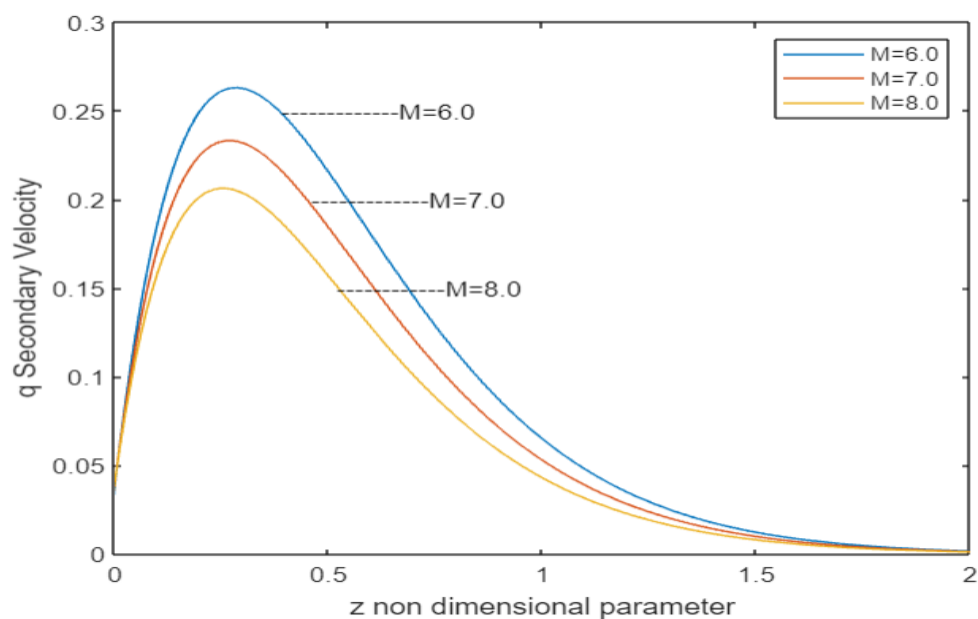


Fig 15 : Secondary Velocity Profiles for the distinctive values of Hartmann number M

It is clearly observable from the diagram that increase in the value of Hartmann number values induces increase in the Secondary velocity and the same is true for all the three values experimented with $M = 6.0, 7.0, 8.0$.

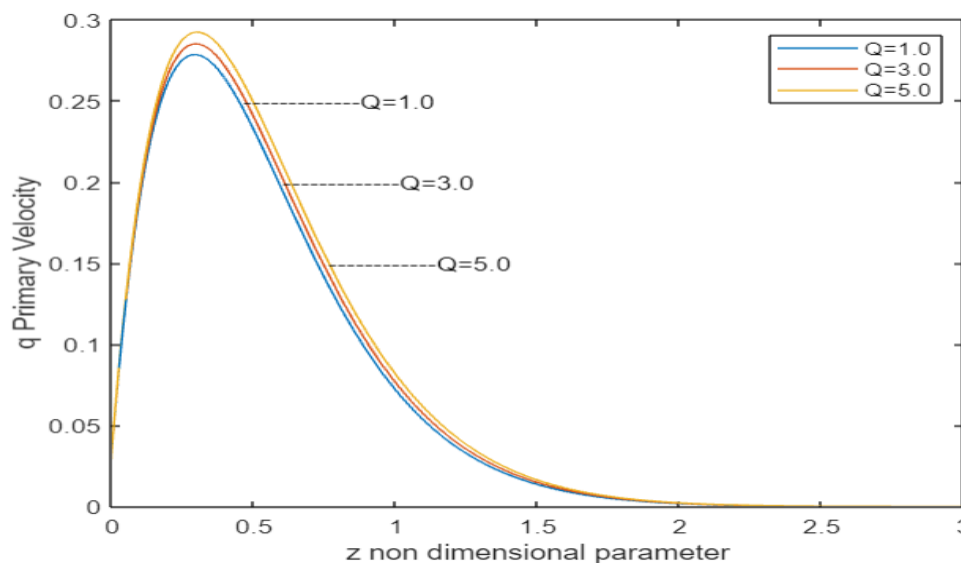


Fig 16 : Primary Velocity Profiles for the various values of Heat Source Q.

It is clearly observable from the diagram that increase in the value of Heat Source Q values induces increase in the Primary Velocity and the same is true for all the three values experimented with $Q = 1.0, 3.0, 5.0$.

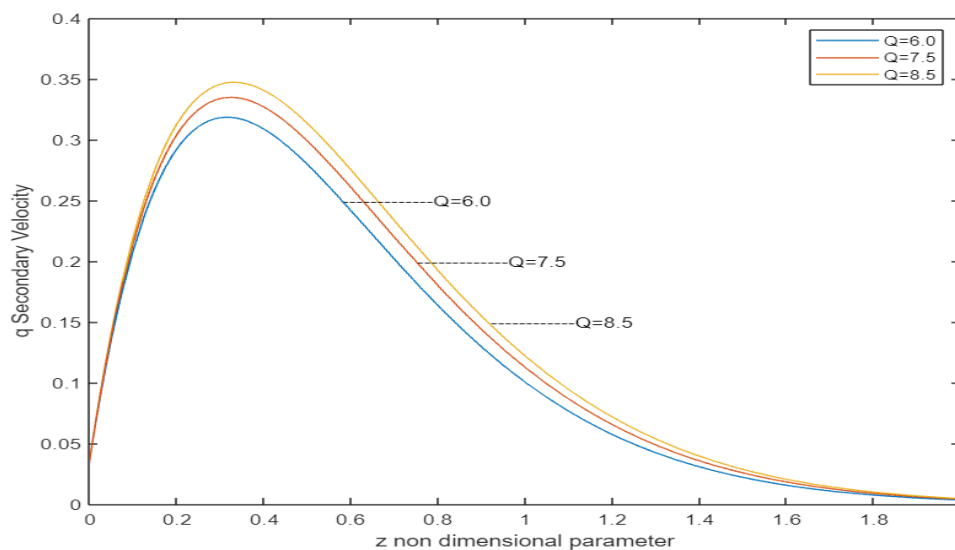


Fig 17 :Secondary Velocity Profiles for the various values of Heat Source Q.

It is clearly observable from the diagram that increase in the value of Heat Source Q values induces increase in the Secondary velocity and the same is true for all the three values experimented with $Q = 6.0, 7.5, 8.5$.

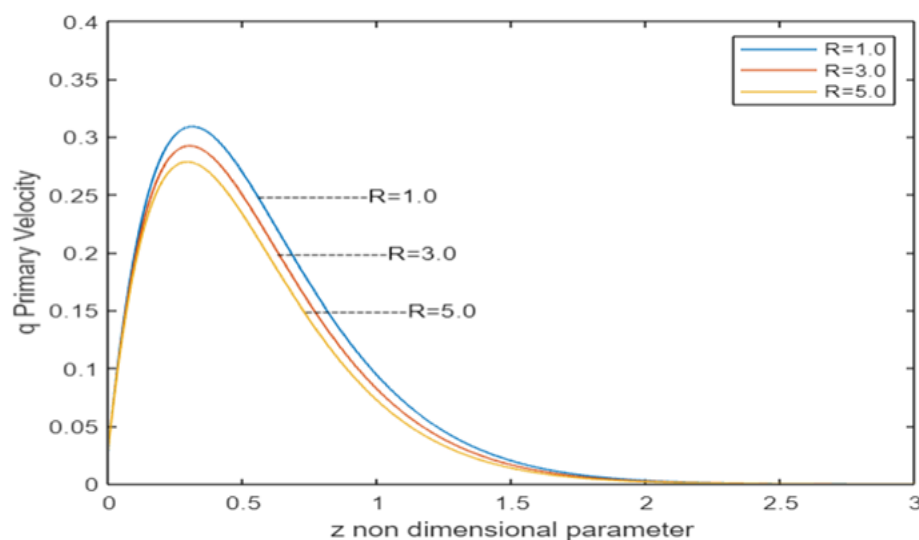


Fig 18 : Primary Velocity Profiles for the various values of Radiation R.

It is clearly observable from the diagram that increase in the value of Radiation values induces declines in the Primary Velocity and the same is true for all the three values experimented with $R = 1.0, 3.0, 5.0$.

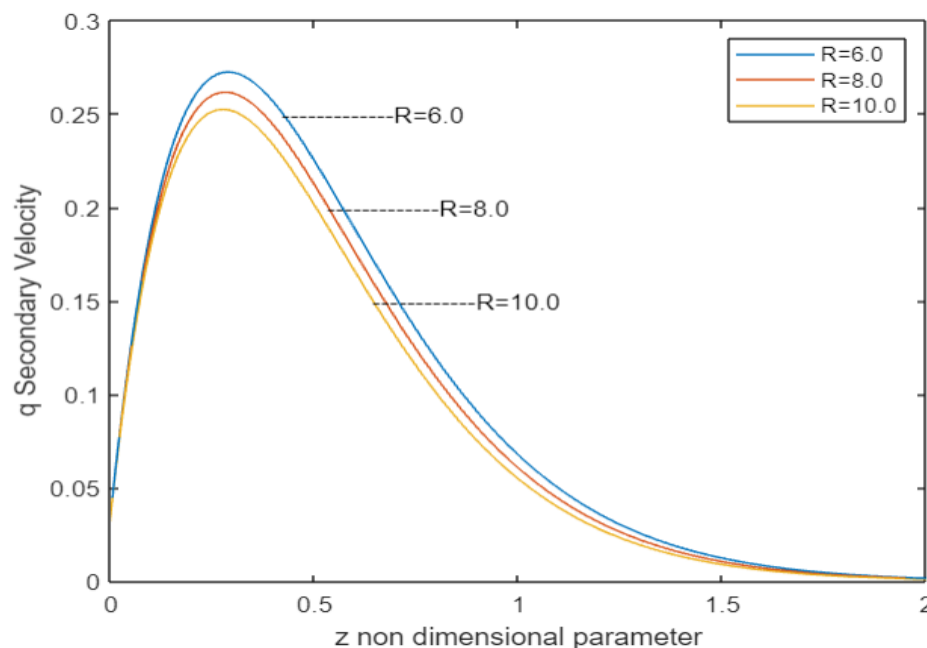


Fig 19 : Secondary Velocity Profiles for the various values of Radiation R.

It is clearly observable from the diagram that increase in the value of Radiation values induces declines in the Secondary velocity and the same is true for all the three values experimented with $R = 6.0, 8.0, 10.0$.

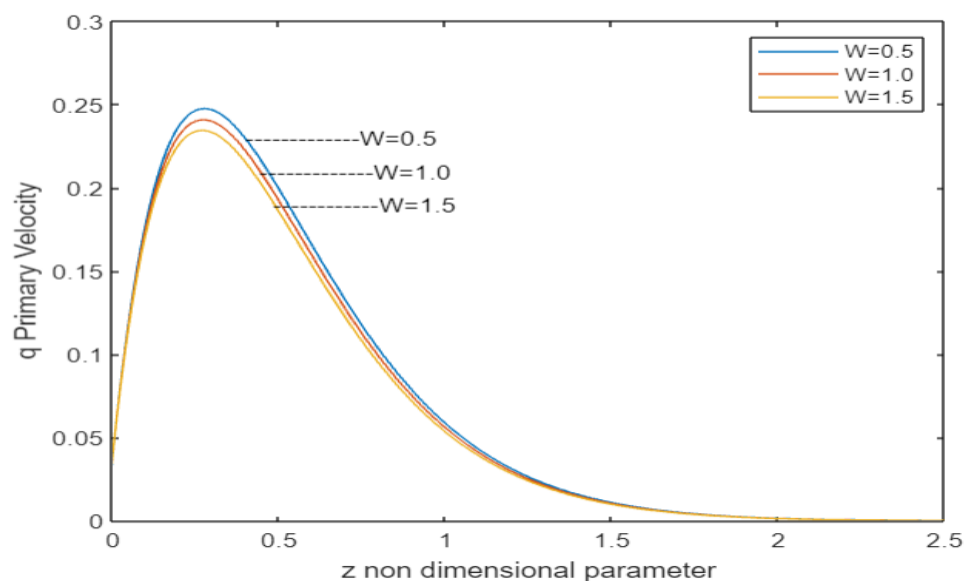


Fig 20 : Primary Velocity Profiles for the distinct values of Rotation W.

It is clearly observable from the diagram that increase in the value of Rotation values induces declines in the Primary Velocity and the same is true for all the six values experimented with $W = 0.5, 1.0, 1.5$.

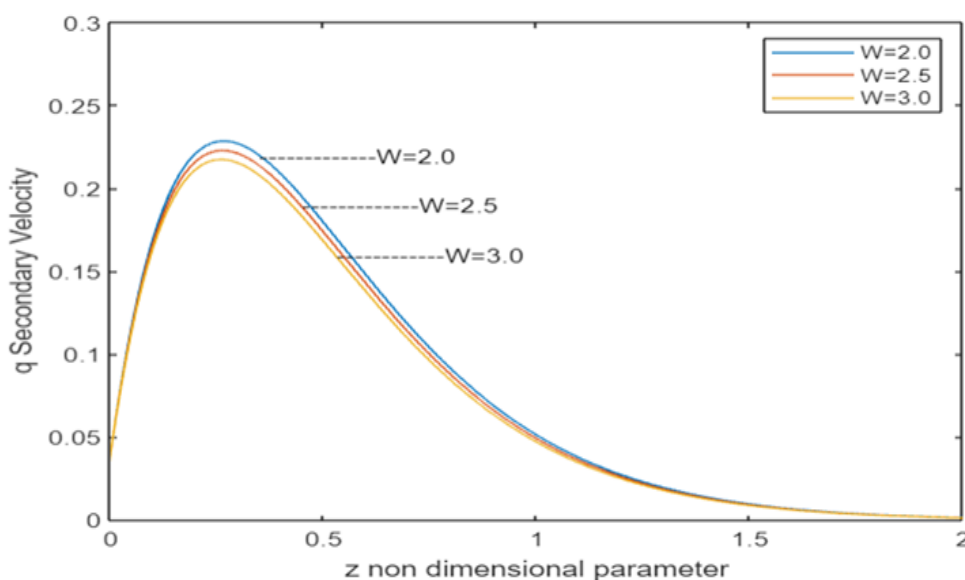


Fig 21 : Secondary Velocity Profiles for the distinct values of Rotation W .

It is clearly observable from the diagram that increase in the value of Rotation values induces declines in the Secondary velocity and the same is true for all the six values experimented with $W = 2.5, 3.0, 3.5$.

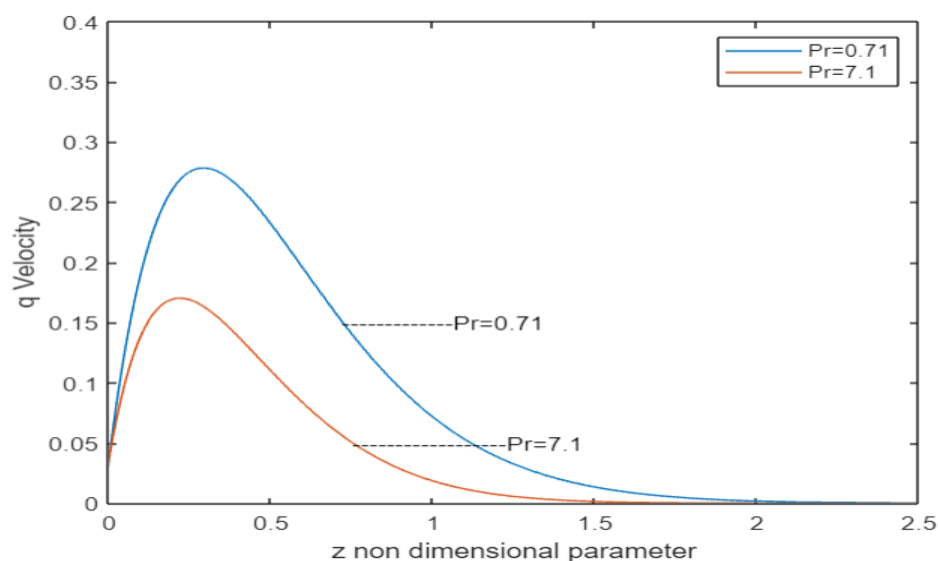


Fig 22 : Velocity Profiles for the Prandtl Number Pr .

It is clearly observable from the diagram that increase in the value of Prandtl values induces declines in the velocity and the same is true for all the values experimented with $Pr = 0.71, 7.0$.

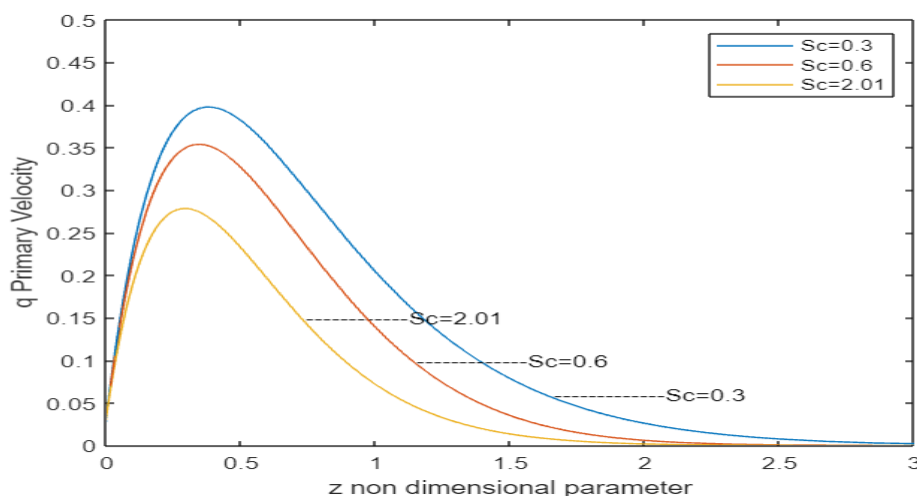


Fig 23: Velocity Profiles for the Schmidt number Sc .

It is clearly observable from the diagram that increase in the value of Schmidt number values induces declines in the Velocity and the same is true for all the six values experimented with $Sc = 0.3, 0.6, 2.01$

5. Tabulation

Table 1. Numerical values for estimated Conc. profiles various k and Sc .

Non-dimensional Parameter	Figure 1	Figure 2
	Concentration k	Concentration Sc
Sc	2.01	0.3,0.6,2.01
k	5,8,11	1
t	0.2	0.2

Table 2. Numerical estimated Temp. profiles values for several values of Pr , R , and Q .

Non-dimensional Parameters	Fig. 3	Fig. 4	Fig. 5
	Temperature Pr	Temperature R	Temperature Q
Pr	0.71,7.0	0.71	0.71
R	5	5,10,15	5
Q	1	1	2,3,4
t	0.2	0.2	0.2

Table 3. Numerical estimated Velocity. Profiles values for several values of Gc and Gr .

Non-dimensional Criteria	Fig. 6	Fig. 7	Fig. 8	Fig. 9
	Primary Velocity Gc	Secondary Velocity Gc	Primary Velocity Gr	Secondary Velocity Gr
Gr	7	7	5,7,10	11,14,17
Gc	5,7,10	11,14,17	7	7
Pr	0.71	0.71	0.71	0.71

R	5	5	5	5
Q	1	1	1	1
M	5.5	5.5	5.5	5.5
h	2	2	2	2
w	1	1	1	1
Sc	2.01	2.01	2.01	2.01
k	1	1	1	1
t	0.2	0.2	0.2	0.2

Table 4. Numerical estimated Velocity profiles values for several values of h and k

Non-dimensional Criteria	Fig10	Fig 11	Fig 12	Fig 13
	Primary Velocity h	Secondary Velocity h	Primary Velocity k	Secondary Velocity k
Gr	7	7	7	7
Gc	7	7	7	7
Pr	0.71	0.71	0.71	0.71
R	5	5	5	5
Q	1	1	1	1
M	5.5	5.5	5.5	5.5
h	1,1.5,2	1.75,2,4	2	2
w	1	1	1	1
Sc	2.01	2.01	2.01	2.01
k	1	1	1,3,5	8,10,12
t	0.2	0.2	0.2	0.2

Table 5. Numerical estimated Velocity. profiles values for several values of Q and R

Non-dimensional Parameters	Fig. 14	Fig. 15	Fig. 16	Fig. 17
	Primary Velocity Q	Secondary Velocity Q	Primary Velocity M	Secondary Velocity M
Gr	7	7	7	7
Gc	7	7	7	7

Pr	0.71	0.71	0.71	0.71
R	5	5	5.0	5.0
Q	1,4,7	5,8,11	1	1
M	5.5	5.5	5,6,7	8,10,12
h	2	2	2	2
w	1	1	1	1
Sc	2.01	2.01	2.01	2.01
k	1	1	1	1
t	0.2	0.2	0.2	0.2

Table 6. Numerical values for estimated Velocity profiles for varying R and W values.

Non-dimensional Parameters	Fig. 18	Fig. 19	Fig. 20	Fig. 21
	Primary Velocity R	Secondary Velocity R	Primary Velocity w	Secondary Velocity w
Gr	7	7	7	7
Gc	7	7	7	7
Pr	0.71	0.71	0.71	0.71
R	0.5,2.5,6	5.5,9.5,17	5	5
Q	1	1	1	1
M	5.5	5.5	5.5	5.5
h	2	2	2	2
w	1	1	0.5,1.0,1.5	2.0,2.5,3.0
Sc	2.01	2.01	2.01	2.01
k	1	1	1	1
t	0.2	0.2	0.2	0.2

Table 7. Numerical values for estimated Velocity profiles for varying Pr and Sc values.

Non-dimensional Parameters	Fig. 22	Fig. 23
	Velocity Pr	Velocity Sc
Gr	7	7
Gc	7	7

Pr	0.71, 7.0	0.71
R	5	5
Q	1	1
M	5.5	5.5
h	2	2
w	1	1
Sc	2.01	0.3,0.6,2.01
k	1	1
t	0.2	0.2

6. Conclusion

As this is a variational study from the literature involving accelerated isothermal vertical plate with the basic HMT aspects, this provides a simple and nice platform for computational work and based on the calculations, we could conclude that

- (i) Velocity reduces when Radiation 'R' rises
Velocity reduces when Hartmann number M rises
Velocity reduces when Rotation Values w rises and
Velocity rises when Grashof 'Gc' and 'Gr' Values rises
Velocity rises when Heat Source 'Q' rises,
Velocity rises when Hall Current 'h' rises
- (ii) Temperature falls when Radiation 'R' rises and
Temperature rises when Heat Source 'Q' rises.
- (iii) Concentration reduces when Chemical reaction 'k' increased.

So, we are able to achieve an extended list of conclusions by the variation and we intend to enhance the study by including more parameters in our future study.

References

- [1] Das, U. N. Deka, R. K., and Soundalgekar, V. M. (1994). 'Effects of Mass Transfer on Flow Past an Impulsively Started Infinite Vertical Plate With Constant Heat Flux and Chemical Reaction'. -Forschungingenieurwesen, Vol 60: pp:284-287.
- [2] Muthucumaraswamy R and Geetha E (2014): *Effects of parabolic motion of an isothermal vertical plate with constant mass flux*- Ain Shams Engineering Journal, Vol.5, pp.1317-1323.
- [3] M.N.Sarki, A. Ahmed (2012):*Heat And Mass Transfer With Chemical Reaction And Exponential Mass Diffusion*-International Journal of Engineering Research &

Technology(IJERT) Vol 1,no 8

[4]M.Thamizhsudar,R.Muthucumaraswamy, A.K. Bhuvaneshwari(2017.) : *Heat and Mass Transfer Effects on MHD Flow Past an Exponentially Accelerated Vertical Plate in the Presence of Rotation and Hall Current* - Jour of Adv Research in Dynamical & Control System Vol. 9, pp: 2.

[5] S.Dilip Jose and A. Selvaraj Convective(2021): *Heat And Mass Transfer Effects Of Rotation On Parabolic Flow Past An Accelerated Isothermal Vertical Plate In The Presence Of Chemical Reaction of First Order* - JP Journal of Heat and Mass Transfer, Vol 24, no 1, pp: 191-206.

[6] R.Muthucumaraswamy, K. Muthuracku Hall *Effects on MHD Flow Past an Exponentially Accelerated Isothermal Vertical Plate with Variable Mass Diffusion In The Presence Of Rotating Fluid*. ANNALS of Faculty Engineering Hunedoara – International Journal of Engineering 229 [Fascicule 4 Tome XIII [2015] – Fascicule 4 [November] ISSN: 1584-2673

[7] J.Uwanta, Murtala Sani. (2014) : *Heat Mass Transfer Flow past an Infinite Vertical Plate with Variable Thermal Conductivity, Heat Source and Chemical Reaction* - The International Journal Of Engineering And Science (IJES) , Vol 3 , pp:77-89

[8]D. Maran, A. Selvaraj, M. Usha and S. Dilip Jose (2021) : *First order chemical response impact of MHD flow past an infinite vertical plate within sight of exponentially with variable mass diffusion and thermal radiation*, Materials Today: Proceedings, Vol 46 pp: 3302 -3307.

[9] K. Rachna (2013) : *Unsteady MHD flow, heat and mass transfer along an accelerated vertical porous plate in the influence of viscous dissipation, heat source and variable suction*- International Journal of Mathematics and Computer Applications Research, Vol 3 no 1, pp:229-236.

[10] M. S. Abel and N. Mahesha (2009) : *Effects of thermal buoyancy and variable thermal conductivity in a power law fluid past a vertical stretching sheet in the presence of non uniform heat source*-International Journal of Nonlinear Mechanics, Vol 44, pp: 1-12.

[11] M. Ferdows, M. A. Sattar and M. N. A. Siddiki (2004) : *Numerical approach on parameters of the thermal radiation interaction with convection in boundary layer flow at a vertical plate with variable suction*, Thammasat International Journal of Science and Technology, Vol 9, pp:19-28.

[12] M. Acharya, G. C. Dash and L. P. Singh (1995) : *Effect of chemical and thermal diffusion with Hall current on unsteady hydromagnetic flow near an infinite vertical porous plate*- Journal of Applied Physics, Vol 28, pp:2455-2464.

[13] P.G. Siddheshwar, U.S. Mahabaleshwar (2005) : *Effect of radiation and heat source on MHD flow of a viscoelastic liquid and heat transfer over a stretching sheet*- Int. J. Non-Linear Mech. Vol 40, pp:807–820.

[14] P. R. Sharma and G. Singh (2008) : *Unsteady MHD free convective flow and heat transfer along a vertical porous plate with variable suction and internal heat generation-* International Journal of Applied Mathematics and Mechanics, Vol 4, pp:1-8.

[15] R.B.Hetnarski *Stosowanie Matematyki VII* (1964). *On inverting the laplace Transforms connected with the error function.* *Applicationes Mathematicae* Vol:7, no 4, pp:399-40.

[16] R. B. Hetnarski (1975): *An algorithm for generating some inverse Laplace transform of exponential form-* ZAMP Vol 26 , pp:249-253.

[17] R.Muthucumaraswamy, (2002): *Effects of a chemical reaction on a moving isothermal vertical surface with Suction - India ActaMechanica* Vol 155, pp:65- 70